Clinical and Experimental Immunology, 2022, **210**, 24–38
https://doi.org/10.1093/cei/uxac058
Advance access publication 8 July 2022
Review

Clinical & Experimental IMMUNOLOGY

OXFORD

Review

In vivo quantitative imaging of hippocampal inflammation in autoimmune neuroinflammatory conditions: a systematic review

P. Nwaubani[1], M. Cercignani[2] and A. Colasanti[1,*]

[1]Department of Clinical Neuroscience and Neuroimaging, Brighton and Sussex Medical School, University of Sussex, Falmer, Brighton, UK
[2]Cardiff University Brain Research Imaging Centre, Cardiff University, Cardiff, UK

[*]Correspondence: Alessandro Colasanti, Department of Clinical Neuroscience and Neuroimaging, Brighton and Sussex Medical School, University of Sussex, Trafford Centre for Medical Research, University of Sussex, Falmer, Brighton, BN1 4RY, UK. Email: a.colasanti@bsms.ac.uk

Abstract

The hippocampus is a morphologically complex region of the brain limbic system centrally involved in important cognitive, affective, and behavioural regulatory roles. It has exquisite vulnerability to neuroinflammatory processes, with some of its subregions found to be specific sites of neuroinflammatory pathology in *ex-vivo* studies. Optimizing neuroimaging correlates of hippocampal neuroinflammation would enable the direct study of functional consequences of hippocampal neuroinflammatory pathology, as well as the definition of therapeutic end-points for treatments targeting neuroinflammation, and their related affective or cognitive sequelae. However, *in vivo* traditional imaging of the hippocampus and its subregions is fraught with difficulties, due to methodological challenges deriving from its unique anatomical characteristics. The main objective of this review is to provide a current update on the characterization of quantitative neuroimaging correlates of hippocampal neuroinflammation by focusing on three prototypical autoimmune neuro-inflammatory conditions [multiple sclerosis (MS), systemic lupus erythematosus (SLE), and autoimmune encephalitis (AE)]. We focused on studies employing TSPO-targeting positron emission tomography (PET), quantitative magnetic resonance imaging (MRI), and spectroscopy techniques assumed to be sensitive to neuroinflammatory tissue changes. We found 18 eligible studies (14, 2, and 2 studies in MS, AE, and SLE, respectively). Across conditions, the largest effect was seen in TSPO PET and diffusion-weighted MRI studies. No study examined neuroinflammation-related changes at the hippocampal subfield level. Overall, results were largely inconsistent due to heterogeneous imaging methods, small sample sizes, and different population studies. We discuss how these data could inform future study design and conclude by suggesting further methodological directions aimed at improving the precision and sensitivity of neuroimaging techniques to characterize hippocampal neuroinflammatory pathology in the human brain.

Summary

The hippocampus is a complex brain region crucially involved in neuroinflammation. We systematically reviewed quantitative imaging studies focusing on hippocampal pathology in autoimmune neuroinflammatory conditions and identified unmet research needs and future methodological directions.

Keywords: hippocampus, neuroinflammation, MRI, neuroimaging, autoimmune

Abbreviations: ALD: Alzheimer's disease; AD: axial diffusivity; ADC: apparent diffusion coefficient; AE: autoimmune encephalitis; ANAM: automated neuropsychological assessment metrics; BBB: blood brain barrier; CA: Cornus Ammonis; CIS: clinical isolated syndrome; CLVT: California verbal learning test; CNS: central nervous system; CSF: cerebro-spinal fluid; DCE: dynamic contrast enhanced; DG: dentate gyrus; DT: diffusor tensor; DW: diffusion-weighted; DVR: distribution volume ratio; EAE: experimental autoimmune encephalitis; EPI: echo-planar imaging; FLAIR: fluid-attenuated inversion recovery; FSL: FMRIB software library; HPA: hypothalamic-pituitary-adrenal; IQT: image quality transfer; LTP: long-term potentiation; MD: mean diffusivity; ML: molecular layer; MRI: magnetic resonance imaging; MRS: magnetic resonance spectroscopy; MS: multiple sclerosis; MTLE: mesial temporal lobe epilepsy; MTR: magnetization transfer ratio; NODDI: neurite orientation dispersion and density imaging; PET: positron emission tomography; PBR: peripheral benzodiazepine receptors; RAVLT: ray auditory verbal learning test; ROCF: Rey–Osterrieth complex figure; RRMS: relapsing remitting multiple sclerosis; SDMT: symbol digit modalities test; SLE: systemic lupus erythematosus; SLM: stratum lacunosum moleculare; SR: stratum radiatum; SUV: standardise uptake values; SPMS: secondary progressive multiple sclerosis; TLE: temporal lobe epilepsy; TSPO: translocator protein; V_T: volume of distribution

Introduction

The hippocampus is a complex limbic structure anatomically embedded in each medial temporal lobe of the cerebral cortex. The functional role of the hippocampus has been well characterized and includes critical roles in learning, memory processes, spatial navigation, regulation of hypothalamic-pituitary-adrenal (HPA) axis function, and modulation of emotional behaviour. Several notable connections in and around the hippocampus are central to these functions. Polysynaptic pathways effectively regulate the learning/

Received 23 November 2021; Revised 17 May 2022; Accepted for publication 4 July 2022

memory loop, and reciprocal and direct projections to the hypothalamus and amygdala via a ventral striatal loop are elemental in influencing motor and emotional behaviour, as well as the release of adrenocorticotropic hormones [1].

The hippocampus is implicated in the orchestration of numerous critically important allostatic processes that facilitate neurodevelopment through the life span, adaptation to challenging environments, and response to stress, as well as insults and injury. These processes include neurogenesis and synaptic plasticity (long-term potentiation, LTP); excitation/inhibition balance and neuronal excitability, and tight and dynamic feedback regulation of HPA axis function. The functional consequences of hippocampal neurodegeneration, the most obvious being seen in neuropsychiatric conditions such as Alzheimer's disease (ALD), have enormous clinical relevance and impact in terms of general functional impairment and disability, reflecting the central role of the above-mentioned critical processes and systems.

Hippocampal pathology has been the subject of extensive preclinical mechanistic characterization. A large body of the experimental animal and histopathological research established that the hippocampus is subject to neuroinflammatory pathology [2, 3] and that hippocampal neuroinflammation can have a direct impact on its main roles and functions, culminating in alterations in neurogenesis such as reduction in synaptic density [4], and alterations in synaptic plasticity [5], indicating plausible mechanisms that underlie cognitive and affective sequelae of neuroinflammatory pathology.

This exquisite vulnerability of the hippocampus to neuroinflammation is related to several converging factors, including its plasticity and involvement in neuroimmune cross-talks [6, 7]. The hippocampal proximity to the choroid plexus for instance is presumed to facilitate, via alterations in CSF composition and CNS inflammatory immune signal processing, activated lymphocytic cell entry during neuroinflammatory pathology [8, 9, 10]. The hippocampus also contains a very high density of interleukin 1 receptors (IL1) which mediate inflammatory processes [11], with the highest expression of IL1 receptors located in the granule layer of the dentate gyrus and pyramidal cell layer (CA1-4) of the hippocampus. Microglia in the hippocampal neuronal system of adult mice have a higher proliferative capability against LPS-induced inflammatory stimulation, relative to other brain regions examined [12].

More so, immune signalling molecules such as cytokines and chemokines, produced within the hippocampus in response to any perturbations of CNS homeostasis, are implicated in normal hippocampal neurogenesis processes [13]. Adult neurogenesis is defined as a process whereby adult neural precursors in the CNS produce functional neurons [14]. Recognized as a continuing process, hippocampal neurogenesis is characterized by the introduction of new neurons in the memory processing circuits and is a vital determinant of the cognitive reserve [15]. The impact of adult hippocampal neurogenesis has consistently been linked to the development of depression and anxiety [16]. Neurogenesis in the subgranular zone of the dentate gyrus (DG) in particular appears to be readily impaired in a transgenic mouse model of neuroinflammation secondary to IL6 overexpression [17]. In a mouse model of experimental autoimmune encephalitis (EAE), these impairments of neurogenesis and neuroplasticity could be linked to specific microstructural modifications in the molecular layer (ML) of the DG, such as alterations in the dendritic tree and decreases in dendritic length, which manifest in diffusion-weighted MRI as reductions in axial diffusivity (AD, i.e. water diffusion along tracts) and mean diffusivity (MD). Interestingly, the reductions were only visible to the ML of DG, and not in other subfields [18], implying subregional variability to neuroinflammatory mechanisms, with potential relevance to the definition of specific anatomical neuroimaging endpoints.

The hippocampus also has high metabolic vulnerability due to limited perfusion reserve. In the presence of cerebral small vessel pathology, the already miniature arterial supply (posterior cerebral and anterior choroidal vessels), especially when only independently supplied (by the posterior cerebral artery) is compromised, leading to hypoxic injury in the hippocampal region [19]. Indeed, when compared to the neocortex, experimental studies indicate notable reductions in blood flow, blood oxygenation, and neurovascular coupling in the hippocampus as a consequence of distinct alterations in endothelial cell function and vascular networks, such as lower capillary density and marginal pericyte contractile morphology [20]. Accordingly, there are observed varying individual subfield vulnerabilities with respect to hypoxic/ischaemic injury. Specifically, CA1 pyramidal neurons are found to be more vulnerable to ischemic effects, due in part to reduced metabolic capabilities and excess glutamate release, compared to other hippocampal subfields [21, 22]. These findings are paralleled by the notion of an extremely high metabolic requirement of a specific subgroup of hippocampal interneurons functioning at the near limit of their mitochondrial metabolic capacity to continuously provide fine-tuning of the neuronal excitatory-inhibitory balance of hippocampal circuits [23]. Considering the increased neurometabolic demands generally associated with neuroinflammatory processes, the sensitivity of the hippocampus to inflammation, and its limited oxygen supply reserve, it would be expected that the hippocampal metabolic vulnerability would be further exaggerated and amplified in neuroinflammatory pathology.

Although abundant animal research provided full characterization of inflammatory pathology of the hippocampus, there has been comparatively less research on the pathological characteristics of human hippocampal neuroinflammation. A few post-mortem studies provide evidence of neuroinflammatory demyelination of the human hippocampus in the prototypical neuroinflammatory condition, multiple sclerosis (MS) [2, 3, 4]. However, no study so far has directly correlated post-mortem pathological findings to neuroimaging, to enable *in vivo* characterization of hippocampal neuroinflammation. The ability to identify neuroimaging biomarkers of hippocampal inflammation *in vivo* would be crucial to characterize its pathology but also would help in the identification of endpoints for clinical trials with therapeutics targeting neuroinflammatory processes.

Over the past two decades, there have been promising advances in the field of quantitative neuroimaging, in terms of sensitivity to detect neuroinflammation. For example, PET targeting 18 kDa translocator protein (TSPO) as well as novel MRI approaches claim to have good sensitivity and some degree of specificity for measuring brain inflammatory processes [24–28]. However, various methodological aspects complicate the characterization of the hippocampus with neuroimaging. For instance, the complex sub structural organization of the hippocampal formation, which comprise subfields, has individual vulnerability to physiological and

pathological processes. Pereira *et al.* [29] observed a correlation between ageing, diffusion tensor imaging measures, and volumes of varying subfields. Zheng *et al.* [30] also observed volume alterations of differing hippocampal subfields at different ages with positive correlations to delayed and immediate recall measures. Specifically, CA1-4 and DG are impacted upon. Indeed, some studies have emphasized distinct links between biological ageing, elevated inflammatory markers, and chronic inflammation, a phenomenon known as inflammageing or accelerated aging [31, 32].

Given the above evidence of aging-related processes impacting differentially on hippocampal subfields, it is plausible to expect similar subfields-specific vulnerability to neuroinflammatory processes. In particular, and as highlighted above; such mechanisms may comprise the interplay between glial activation and the rate of neurogenesis in DG and under perfusion-induced metabolic modifications made more prominent in CA1.

The unique anatomical location of the hippocampus also makes it vulnerable to partial volume artefacts (when more than one tissue type is present in a voxel, invalidating the quantitative accuracy). The use of segmentation techniques employing automated co-registration of quantitative maps on high-resolution anatomical images might therefore be suboptimal. Further, separation of subfields is difficult due to the low resolution of imaging techniques. Conventional MRI approaches have also failed to accurately discriminate between varying subfield layers.

Despite these challenges associated in general with hippocampal neuroimaging methods, there has been an increasing number of applications of novel quantitative approaches to study neuroinflammation in the hippocampus. In the present overview, we will provide details on how these quantitative techniques might inform various aspects of neuroinflammatory pathology. We also aim to summarize the state of the art in hippocampal imaging of neuroinflammation by systematically reviewing studies that employed quantitative imaging techniques to assess hippocampal neuroinflammatory processes. We will focus on MS, systemic lupus erythematosus (SLE), and autoimmune encephalitis (AE) as prototypical examples of autoimmune neuroinflammatory diseases that might involve the hippocampus. We include studies that used imaging techniques targeting neuroinflammation-specific pathological processes, namely:

(1) the activation of resident immunocompetent cells (TSPO PET; MRS (lactate, myo-inositol, choline);
(2) BBB disruption/permeability (dynamic contrast enhanced or DCE MRI);
(3) Interstitial modifications consequent to neuroinflammation, such as oedema and modifications to the relative size of the extra-cellular water compartment, which can be detected using diffusion-weighted (DW) MRI, magnetization transfer ratio (MTR), or magnetic resonance spectroscopy (MRS) by quantifying metabolites such as lactate, choline, and lipids.

Furthermore, we will also separately report findings from quantitative neuroimaging studies that assessed hippocampal morphology differentially across hippocampal subfields. These studies will be useful to reveal the sequelae of neuroinflammation such as neuronal loss/neurodegeneration.

Overview of relevant imaging techniques

The most frequently used imaging tool in routine clinical settings to identify *in vivo* biomarkers in neuroinflammatory conditions such as MS, is MRI. For example, MRI is established as a gold standard in the diagnosis of MS and is used to investigate the natural course of the disease and monitor treatment effects in clinical trials. MRI "lesions" appear as hyperintensities on T2-weighted images and, in the relapsing-remitting phase of MS (RRMS), the effect of a treatment on MRI lesions and its effect on the frequency of relapses are strongly correlated, supporting the use of MRI parameters as surrogates for clinical end-points [33]. However, conventional MRI measures are limited by lack of neuropathological specificity, and for example, non-specifically reflect demyelination, oedema, or gliosis [34]. Furthermore, as disability progresses in the secondary progressive phase of MS (SPMS), the strength of the relationship between T2-hyperintensities and clinical severity becomes weaker. Importantly, conventional MRI measures, including T2-weighted FLAIR, are only able to detect a minority of cortical or sub-cortical grey matter lesions. This may be due to the different pathophysiology of cortical grey matter lesions, compared to those in the white matter, with less inflammatory cell infiltration and absent blood–brain barrier damage [35]. All these factors impact the value and utility of conventional MRI measures for the assessment of hippocampal neuroinflammation. We have therefore focused our review on alternative molecular imaging techniques that provide higher, although not absolute, specificity to the pathological processes that are relevant for hippocampal neuroinflammation. Here we provide a brief description of the imaging techniques used in the studies we reviewed.

Positron emission tomography

Positron emission tomography imaging, based on the *in vivo* administration of radiolabelled ligands that bind selectively to a target of interest, offers the potential of high specificity for molecular markers of cellular and metabolic processes. The high selectivity of PET allows microdosing of the radiotracer, ensuring high safety and tolerability for the subjects who undergo the procedure. Although for over two decades there have been intense research in the identification of suitable PET targets for neuroinflammation imaging, only a limited number of targets have been investigated in living patients to date, and the only extensively characterized target in clinical populations is the 18 KDa translocator protein (TSPO). TSPO, formerly known as the peripheral benzodiazepine receptor (PBR), is a protein primarily (but not exclusively) localized on cells outer mitochondrial membrane. In normal conditions, TSPO is highly expressed in peripheral tissues, particularly where steroids are synthesized, consistent with its role in steroidogenesis [36]. In the normal human brain, the expression of TSPO is low. TSPO expression is observed in macrophages and microglia, astrocytes, oligodendrocytes, endothelial cells and smooth muscle cells, platelets, subpial and subependymal glia, meninges (vessels, macrophages and sometimes, arachnoid cells), ependymal cells, and choroid plexus. Furthermore, recent evidence confirmed that TSPO is also expressed in neurons [37, 38]. Autoradiography studies using radiolabelled TSPO ligands demonstrate that the expression of TSPO is dramatically enhanced in response to microglia proliferation or activation,

in the case of a disrupted blood-brain barrier, on invading cells of a mononuclear-phagocyte lineage [39–42]. The precise role of TSPO in the inflammatory processes of microglia during such disease states remains unclear, with accumulating evidence suggesting an allostatic role of TSPO in the orchestration of bioenergetic, and more specifically, redox responses that accompany neuroinflammatory processes.

In neuroinflammation, the areas of focal tissue damage and demyelination, such as for example in active or chronic active MS lesions, are characterized by dramatically increased microglia density, therefore TSPO represents an attractive target for imaging focal lesional neuroinflammatory pathological processes. However, TSPO PET also enables the assessment of neuroinflammation in non-lesional areas providing clinically relevant information that is not available with conventional routine MRI approaches [25]. An important caveat to consider relates to the notion that the specificity of TSPO to each cellular type is not uniform across species, brain regions, and disease processes [41, 42, 36, 38]. Therefore, the application of TSPO PET imaging should be informed by histopathological studies that reveal, for each specific target and application, which cellular types, and immunopathological processes are contributing the greatest proportion of TSPO signal. In parallel to developments in the TSPO PET field, we note promising results from first-in-human applications of other emerging PET radiotracers targeting neuroinflammatory processes, such as for example the COX-1 targeting [^{11}C] PS13 which displays exquisitely high hippocampal uptake [43]. Furthermore, promising data are emerging from novel human applications of [^{11}C]-deuterium-L-deprenyl ([^{11}C]-DED) [44] and [^{11}C]-BU99008 [45], which bind respectively to Monoamine Oxidase B, and the non-adrenergic imidazoline-2 binding site, both of which are overexpressed in reactive astrocytes.

Magnetic resonance spectroscopy

MRS aims to quantify the concentration of tissue metabolites, by exploiting a phenomenon known as chemical shift. In molecules more complex than water, the negatively charged electrons can oppose the external static magnetic field resulting in a small shift of the resonance frequency of each metabolite. As these molecules are fairly mobile, their signal results in relatively narrow peaks in frequency, which can be easily identified. By measuring the area under each peak, it is possible to estimate their concentration. The main metabolites visible in the brain are N-acetyl aspartate (NAA), only present in neurons, and often regarded as a neuronal marker; choline (Cho), a marker of membrane turnover, which resides in glial cells and neurons; and creatine (Cr), a marker of cellular energetics, often used as a reference for other peaks. Other metabolites interests, which are, however, more difficult to measure, are glutamate (Glu), glutamine (Gln), myo-inositol (mI), and lactate (Lac). The last two are of interest in the context of neuroinflammation, as mI is only present in glial cells, while Lac is virtually invisible in a healthy brains but increases in conditions of hypoxia, poor perfusion, and other pathologies. More details can be found in [46].

Dynamic contrast-enhanced magnetic resonance imaging

The aim of DCE MRI is to assess the integrity of the blood-brain barrier (BBB) by measuring the distribution of a paramagnetic contrast agent (typically, gadolinium chelates) injected intravenously. When the BBB is intact, the contrast agent stays in the vasculature, while in the presence of increased permeability, it leaks into the tissue altering the MRI signal. Alterations to the BBB are known to occur in the presence of neuroinflammation, for example in acute MS lesions [47]. More subtle increases in permeability have also been reported in conditions such as dementia [48], and have been linked to the presence of underlying chronic inflammation. The transfer constant K_{trans} can be estimated by fitting analytical models of tissue compartmentalization to serial T1-weighted acquired after the injection. K_{trans} tends to increase with increased BBB permeability. Please see [49, 50] and Fig. 1; for more information.

Diffusion-weighted magnetic resonance imaging

Diffusion refers to the microscopic random motion of small particles immersed in a fluid. Water molecules experience self-diffusion, i.e. diffusion within the water itself. In biological tissue, water self-diffusion is affected by the microstructure, i.e. membranes and organelles that hinder the diffusion of molecules, thus providing information about the microstructure and integrity of the tissue itself. Diffusion-weighted (DW) MRI uses magnetic field gradients to enhance the natural sensitivity of MRI to motion and enables the estimation of tissue apparent diffusion coefficient (ADC) [51]. When it became obvious that diffusion is anisotropic in the white matter, i.e. that it depends on the direction along which it is measured, diffusion tensor (DT) MRI was introduced [52], enabling the estimation of diffusion fractional anisotropy (FA), as well as of the local tissue orientation. The concept of ADC was replaced by the mean diffusivity (MD), a directional average of the diffusion coefficient. MD tends to increase whenever there is an increase in free water content (or loss of tissue), while FA tends to reduce under similar circumstances. Radial (RD) and axial (AD) diffusivities are sometimes used to map diffusion across and along fibre bundles, which have supposedly better specificity to myelin and axon integrity, respectively [53]. Although DT MRI is still extremely popular in clinical applications, more refined models of diffusion MRI, accounting for multiple water compartments, have been introduced. These methods typically require longer acquisition times, which makes them less suited for clinical studies. A good compromise between complexity and acceptable scan time is neurite orientation dispersion and density imaging (NODDI) [54], which provides an estimate of the intra-neurite and the isotropic volume fractions. Although non-specific to inflammation, changes to diffusion parameters such as the mean diffusivity can be the consequence of increased water (oedema), and therefore reflect inflammation.

Magnetization transfer imaging and the magnetization transfer ratio

MRI is only sensitive to the signal from small, mobile hydrogen-containing molecules, as the signal from larger ones (lipids, proteins) decays too fast to be probed. Nevertheless, hydrogen protons in differing chemical environments can exchange magnetization, thus enabling the indirect probing of macromolecular protons through an MRI measurement. This forms the basis of magnetization transfer (MT) imaging. MT uses radiofrequency pulses far from the resonance frequency of water to saturate macromolecular protons without

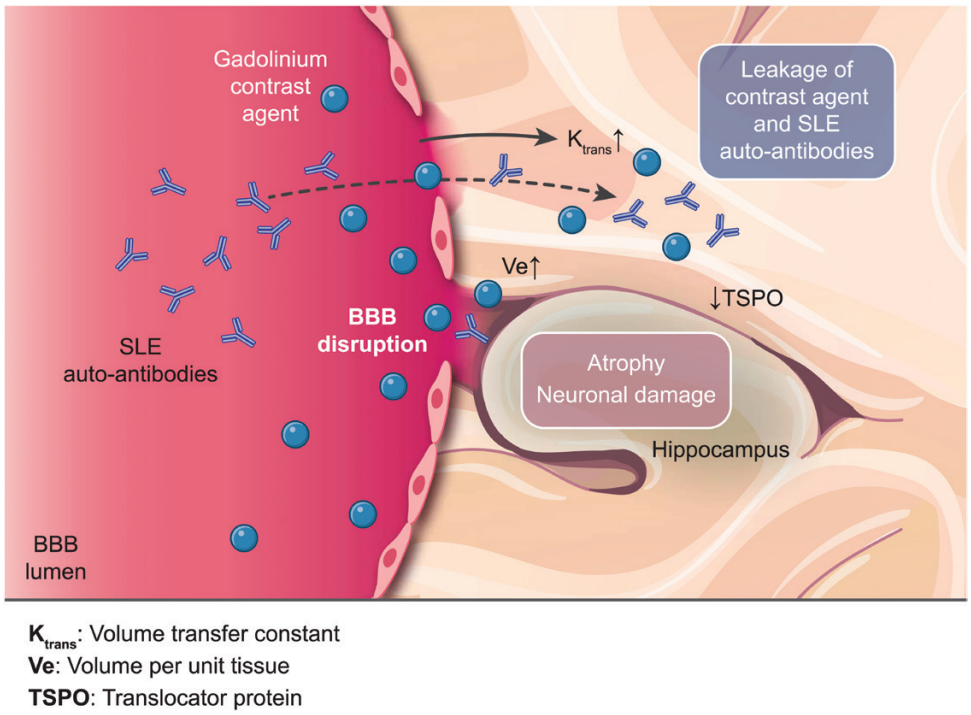

Figure 1: Immunopathology of BBB disruption in SLE. Diagrammatic representation showing rationale for dynamic contrast enhanced MRI of Neuropsychiatric lupus pathology with impact on the hippocampus. Neuronal damage within the hippocampus is induced following breach of the blood-brain barrier (BBB) and access of SLE auto-antibodies. Accumulation of gadolinium-based contrast agent, as measured by increasing capillary permeability (K_{trans}), and accumulation in the extravascular space (V_e) have been reported [50]. Significant decrease in TSPO distribution in the hippocampus has also been reported using PET [88].

affecting water protons directly. Thanks to the exchange of magnetization between the two, such saturation is transferred to the water protons and results in a signal attenuation, which depends on the local density of macromolecules. Early attempts to quantify these effects led to the development of the MT ratio (MTR), a percentage difference between the signal measured with and without MT saturation. Larger MTRs typically indicate tissue rich in protein and lipids (including myelin), while reduced MTR values suggest either a reduction in macromolecular content or an increase in the extracellular water compartment. The interested reader is referred to [55]. In rodent, MT imaging has demonstrated sensitivity to the effects of peripheral inflammation on the brain [56] and sciatic nerve [57], primarily through its sensitivity to increased water content.

Mesh modelling

Three-dimensional renderings of brain structures also known as mesh models can be obtained from structural MRI data via finite element modelling. These digital 3D-renderings are obtained by combining simple elements (typically tetrahedral or hexahedral ones). The advantage of mesh models is that they enable relevant properties of the brain, such as cortical folding and structural shape, to be captured better than using standard image volumes. Several image analysis packages include similar options and are typically used to compare morphological structures within or between groups [58]. In the context of hippocampal inflammation, mesh modelling can be used to compare the hippocampal shape and volumes, as well as those of its subfields.

Methods

A systematic review was conducted following PRISMA guidelines (see Supplementary Fig. 1) [59].

Study selection

Prior to the review, we defined our search terms and data to be extracted as highlighted in Supplementary Tables S1 and S2. We employed the free search engine pubmed.ncbi.nlm.nih.gov to search the literature from June 1988 to July 2021. Start year was selected based on when selected articles began to meet relevant criteria as per PubMed search. We also manually searched the references of relevant and related articles. In terms of target clinical populations, we decided to focus our search of studies on quantitative neuroimaging measures of hippocampal neuroinflammation with a focus on three prototypical neuroinflammatory autoimmune conditions for which post-mortem pathology reports clearly confirm hippocampal involvement namely MS; AE; SLE [2, 60, 61, 62]. Eligible studies were then further split into two categories; the first group (15 studies in total) comprised studies that used imaging techniques to target primary neuroinflammatory processes, and the second group (three studies in total) included studies of morphological alterations of hippocampal subfields reflecting neuroinflammatory sequelae, such as neuronal loss/neurodegeneration. We did not include studies focused on conditions such as temporal lobe epilepsy (TLE) and Alzheimer's disease (ALD) with well-characterized hippocampal involvement but whose primary pathology is non-neuroinflammatory. From the selected studies, we reported on each ability to differentiate between patients and normal brain.

Article selection

All articles included are original research papers and are all in the English language. The study designs of selected articles comprised longitudinal studies, case controls, and cross-sectional studies. A primary search was conducted by PN, and reviewed by AC and MC. Only studies, which were eligible, based on inclusion and exclusion criteria were selected.

Data extraction

Data were extracted by PN and later reviewed by AC and MC. Key data included clinical population, imaging methods, outcome measures, and effect sizes. Effect sizes were estimated by calculating Cohen's *d*, which was determined by calculating the mean difference between two groups (affected participants and controls), and dividing obtained result by the standard deviation. Cohen's $d = (M_2 – M_1)/SD$. A complete table of data information is available in Supplementary Table S2.

Quality assessment

The quality of each study included was independently assessed by AC and MC.

Results

During the initial search, we came up with 621 articles (see Prisma flow diagram in Fig 2). We excluded conference extracts, non-human studies and non-English language articles. Case reports, case series, and reviews were also removed. A further 551 articles were excluded upon review of their titles and abstracts. The remaining 29 articles were further screened by three reviewers (PN, AC, and MC): 4 articles were excluded due to imaging methodology not meeting eligibility criteria and a further 7 were excluded because their target disease was not primary neuroinflammatory pathology. A total of 18 studies met the criteria for inclusion. Fifteen of these used imaging techniques directly examining neuroinflammatory pathology, whilst three applied imaging techniques measuring morphological changes in separate hippocampal subfields, reflecting neurodegenerative changes such as neuronal loss secondary to neuroinflammation.

Of the 18 studies included in the systematic review, 14, 2, and 2 studies focused on MS, AE, and SLE respectively. The overall study cohorts included 729 MS, 16 SLE, and 166 patients with autoimmune encephalitis, giving a total number of 911 patients. Healthy controls were 497 in total. Ages ranged from 28 to 66 years and SD between 4 and 13. The female to male ratio was 467/262 for MS patients, and 101/65 for AE patients. The gender of participants was unspecified in the SLE studies. Comprehensive details of demographics and results can be found in Tables 1 and 2. In our review of studies ($n = 15$) targeting primarily neuroinflammatory processes, four studies used TSPO PET, eight studies used DW MRI, whilst one study used DCE, MRS, and MTR, respectively. There was high heterogeneity in terms of techniques and specific imaging methodology employed, and virtually no study replicated exactly the same methodology within the same condition, with the exception of five studies in MS that all used DW MRI. The three PET studies in MS used three different 2nd generation TSPO radiotracers and reported different outcome measures (SUV_R; V_T; and DVR)

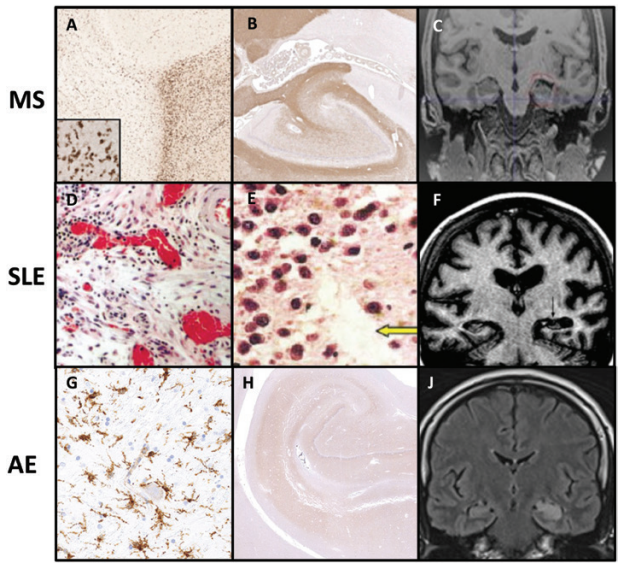

Figure 2: Immunopathological and neuroimaging features of hippocampal neuroinflammation across neuroinflammatory diseases. A, B, C: multiple sclerosis (MS): reduced density of ramified microglia (HLA class II staining) in a lesion centre with increased density of activated microglia and macrophages in the lesion edge (A); pattern of hippocampal demyelination in the DG of a MS patient (B) (from Papadopolous *et al.*, 2009 [2]). Reduced hippocampal volume in patient with MS (C) (unpublished data). D, E, F: systemic lupus erythemateous (SLE): lymphocytes infiltrates in the choroid plexus (D). Evidence of neuronal loss in DG (E) (from Ballok *et al.*, 2004). Hippocampal atrophy in SLE patient (F) (from Appenzeller *et al.* [89]. G, H, J: Autoimmune enkephalitis (AE): hippocampal microglial activation (HLA class II staining) (G) and reduced NMDAR-expression (H) in a patient with NMDAR encephalitis (from Zrzavy *et al.* [90]). FLAIR MR image showing hyperintense swelling of the left hippocampus (J) (from Dekeyzer *et al.* [91]).

All neuroinflammation—targeting studies revealed at least one significant signal change in the hippocampus, relative to the control group. The effect sizes varied greatly across studies (range 0.1–1.6). Across conditions, the largest effect sizes were seen with TSPO PET and DW MRI, indicating respectively increases in hippocampal TSPO binding and in the diffusion-based MD parameter; and a reduction in diffusion-based FA. These changes appeared consistent across MS studies and were evident in various MS sub-types, although the increase in TSPO PET signal [63, 25], as well as changes in diffusion FA and MTR appeared more prominent in progressive forms of MS relative to relapsing-remitting, and even more to CIS [64, 65, 66]. Increases in MD were reported in the two studies on AE [67, 68], which were consistent with findings in MS. In contrast, the two studies in SLE revealed TSPO binding changes opposite to those seen in MS, and alterations in BBB permeability that no other studies had examined. Only two studies (both DW MRI studies on AE) separately examined individual hippocampal subfields [67, 68]. No other studies reported regional subfield analysis.

In MS, increased TSPO binding and elevations in the mean diffusivity parameter (MD) correlated with neurological disability and impaired cognitive performance. For instance, symbol digit modalities test (SDMT) *z*-scores negatively correlated with TSPO uptake in the hippocampus [63]. An increase in diffusion-based MD parameters also negatively correlated with SDMT and California Verbal Learning Test

Table 1: Summary of neuroimaging studies reporting neuroinflammatory changes in the hippocampus

Authors; year	Clinical population		Imaging methods			Outcome measures		Findings	
	Disease	*n* cases; mean age (SD); gender	Imaging type	Segmentation method	Sub-fields	Imaging	Affective/ cognitive	Difference cases vs. controls effect size (ES); p value	Correlations to cognitive/ affective measures
Colasanti *et al.* 2016 [25]	MS	*MS*: *n* = 11; 45(8) yrs; 10F *HC*: *n* = 22; 49(10) yrs; 14F	TSPO PET [^{18}F] PBR111	Automated (CIC Atlas)	No	[^{18}F]PBR111 DVR (cortical GM as pseudo-reference region)	BDI-II	MS: [^{18}F]PBR111 DVR: 0.8 (P = 0.024)	MS cohort: [^{18}F]PBR111 DVR (P = 0.037) pos correl to BDI
Herranz *et al.* 2016 [63]	MS	*RRMS*: *n* = 12; 43(10) yrs; 10F *SPMS*: *n* = 15; 52 (7) yrs; 11 F HC: *n* = 14; 48 (13) yrs; 6 F	TSPO PET [^{11}C] PBR28	Automated (First/FSL)	No	[^{11}C]PBR28 $SUV_{R;}$ DVR	SDMT; TMT-A & B; CVLT-II; BMVT-R; WCST	RRMS: [^{11}C]PBR28 $SUV_{R;}$: 1.1 (P = NS) [^{11}C]PBR28 DVR: 0.8 (P = NS) SPMS [^{11}C]PBR28 $SUV_{R;}$: 1.6 (P < 0.003) [^{11}C]PBR28 DVR: 1.2 (P < 0.005)	Whole MS cohort: [^{11}C] PBR28 SUVR (P = 0.05) neg correl to SDMT
Singhal et al. 2019 [85]	MS	*RRMS*: *n* = 7; 33 (7) yrs; 5 F *SPMS*: *n* = 5; 55(4) yrs; 3F *HC*: *n* = 5; 38 (13) yrs; 3F	TSPO PET [^{18}F] PBR06	Automated (PNEURO)	No	[^{18}F]PBR06 SUV_R	No	MS: [^{18}F]PBR06 $SUV_{R;}$: 1.4 (P = 0.03)	NA
Cappellani *et al.* 2014 [64]	MS	RRMS: *n* = 210; 46(9) yrs; 149 F PMS: *n* = 75; 49 (7) yrs; 57 F HC: *n* = 110; 47 (13) yrs; 76 F	DW-MRI	Automated (First/FSL)	No	FA, MD, RD, AD	No	RRMS: FA 0.4 (P = 0.047) MD 0.6 (P < 0.001) AD 0.5 (P < 0.001) RD 0.6 (P < 0.001)) PMS: FA 0.3 (P = 0.047) MD 0.7 (P < 0.001) AD 0.6 (P < 0.001) RD 0.7 (P < 0.001))	NA
Geurts *et al.* 2006 [74]	MS	MS: *n* = 33; 48 (12) yrs; 16 F HC: *n* = 10; 43 (9); 7 F	MRS	NS	No	Ins	BRB-N	MS: Ins 0.7 (P < 0.05) SPMS Ins 0.9 (NS)	No correlation with BRB-N

Table 1. Continued

Authors; year	Clinical population		Imaging methods			Outcome measures		Findings	
	Disease	*n* cases; mean age (SD); gender	Imaging type	Segmentation method	Sub-fields	Imaging	Affective/ cognitive	Difference cases vs. controls effect size (ES); p value	Correlations to cognitive/ affective measures
Planche *et al.* 2017 [65]	MS	CIS: *n* = 37; 37(10) yrs; 29F MS: *n* = 32; 0.41 (6) yrs (SD); 23 F HC: *n* = 36; 0.38 (10); 24 F	DW-MRI	Automated (first/FSL)	No	MD, FA	SDMT, WAIS-III, SRT, CVLT, BDI	CIS: FA: 0.5 ($P < 0.050$) MS FA: 1.05 ($P < 0.0001$) MD: 1.21 ($P < 0.0001$)	CIS MD CVLT/SRT (DR) $r = -0.57$ ($P = 0.0002$) MS FA SDMT $r = 0.36$ ($P = 0.004$)n.s[a] MD SDMT $r = -0.52$ ($P = 0.002$) ($P = 0.012$)[a]
Roosendaal *et al.* 2010 [86]	MS	MS: *n* = 25; 39 (8) yrs; 17 F HC: *n* = 30; 41 (10) yrs; 20 F	DW-MRI	Automated (first/FSL)	No	MD	LLT, HADS-A, HADS-D,	MS MD LH: 0.7 ($P = 0.01$) MD RH: 0.5 ($P < 0.03$)	NA
Shen *et al.* 2014 [69]	MS	RRMS: *n* = 15; 38 (12) yrs; 11 F HC: *n* = 15; 37 (13) yrs; 11 F	DW-MRI	Automated (first/FSL)	No	FA	HAMD	MS FA: ES ($P < 0.05$)	MS LH FA HAMD $r = 0.5742$ ($P = 0.025$)
Vrenken *et al.* 2007 [66]	MS	RRMS: *n* = 35; 39(7) yrs; 24 F PPMS: *n* = 12; 58(6) yrs 5 F SPMS: *n* = 19; 44 (11) yrs; 11 F HC: *n* = 23; 31 (7) yrs; 11 F	MRI-MTR	Automated (first/FSL)	No	MTR	PASAT	RRMS: MTR 0.1 (*P*=NS) PPMS: MTR 0.7 (*P*=NS) SPMS: MTR 0.9 ($P < 0.05$)	No observed corr.
Yin *et al.* 2018 [87]	MS	MS-SSCI: *n* = 22; NS (7) yrs; 13 F HC: *n* = 22; NS (13) yrs; 13 F	DW-MRI	SPM8	No	FA, ADC	NA	MS-SSCI: RH FA0.1 ($P = 0.042$) LH FA1.4 ($P = 0.000$) MS-SSCI: RH ADCES ($P = 0.047$) LH ADCES (P = NS)	NA

Table 1. Continued

Authors; year	Clinical population		Imaging methods			Outcome measures		Findings	
	Disease	*n* cases; mean age (SD); gender	Imaging type	Segmentation method	Sub-fields	Imaging	Affective/ cognitive	Difference cases vs. controls effect size (ES); p value	Correlations to cognitive/ affective measures
Filip *et al.* 2020 [73]	MS	MS: *n* = 10; 47(12) yrs; 8 F HC: *n* = 10; 46 (13) yrs; 8 F	DW-MRI and susceptibility	Automated (FreeSurfer)	No	RAFF4, T1p, $T2_{p,}$ FA, MD, AD, RD	SDMT CES-D	MS: RAFF4: 1.6 (P = 0.007) T1p: 1.1 (P = 0.041) $T2_{p}$: 1.5 (P = 0.004) FA: 0.6 (P = NS) MD: 1 (P = 0.099) AD: 0.5 (NS) uncorr RD: 1.1 (P = 0.0184) uncorr	No observed correl
Chi *et al.* 2019 [50]	SLE	SLE: *n* = 6; 38(13) yrs; (NS) F HC: *n* = 5; 0.34 (11) yrs;. (NS) F	DCE-MRI	No	No	K^{trans}, Ve, CBF	ANAM, BDI, STAI	SLE: K^{trans}: 0.9 (P = 0.04) Ve: 0.9 (P = 0.04) CBF: 1.1 (P = 0.013)	3 SLE had elevated DNRAB titres with pos correl to BDI, STAI. neg correl to ANAM (not stat sig)
Wang *et al.* 2017 [88]	SLE	SLE (*n* = 10; 41(9) yrs; (NS) F HC (*n* = 11; 39 (11);. (NS) F	TSPO PET [^{11}C]DPA-713	Automated (FreeSurfer)	No	[^{11}C]DPA-713 V_T	ANAM	SLE: [^{11}C]DPA-713 $V_{T;}$: 0.8 ($P < 0.05$)	NA
Finke *et al.* 2016 [67]	Anti-NMDAR Encephalitis	anti-NMDAR encephalitis (*n* = 40; 28(12) yrs; 36 F HC (*n* = 25; 28 (11) yrs; 23 F	DW-MRI	Automated (First/FSL)	Yes	MD	RAVLT, ROCF	Anti-NMDAR Encephalitis: LH MD0.09 (P = 0.004) RH MD 0.7 (P = 0.019)	RAVLT LH MD r = −0.524 (P = 0.001) RH MDr = −0.470 (P = 0.004) ROCF LH MD r = −0.45 (P = 0.008) RH MDr = −0.44 (P = 0.009)
Finke *et al.* 2017 [68]	Anti-LGI1 Encephalitis	Anti- LGI1 encephalitis (*n* = 30; 66(12) yrs; 11 F HC (*n* = 27; 64 (2) yrs; 9 F	DW-MRI	Automated (FreeSurfer)	Yes	MD	RAVLT, ROCF	Anti- LGI1 encephalitis: LH MD1.1 (P = 0.001) RH MD 1 ($P < 0.001$)	RAVLT LH MD r = −0.41 (P = 0.04) RH MDr = 0.57 (P = 0.03)

Table 2: Neurodegenerative changes associated with inflammation in hippocampal subfields

Authors; year	Clinical population		Imaging methods			Outcome Measures		Findings	
	Disease	*n* cases; mean age (SD); gender	Imaging type	Segmentation method	Subfields analysis	Imaging	Affective/ Cognitive	Difference cases vs. controls effect size (ES); *P* value	Correlations to cognitive/ affective measures
Heine *et al.* 2020 [72]	MS Anti-NMDAR encephalitis Anti-LGI1 encephalitis	RRMS (*n* = 30;.43 (6) yrs (SD); 18 F HC (*n* = 30; 0.42 (8); 0.18 F anti-NMDAR encephalitis (*n* = 30; 0.28 (8) yrs (SD); 26 F HC (*n* = 30; 0.29 (8); 0.26 F anti-LGI1 encephalitis (*n* = 30; 0.66 (9) yrs (SD); 9 F HC (*n* = 30; 0.63 (10); 0.9 F	MRI	Automated (first/FSL)	Mesh modelling	Post MRI: Surface based analysis: Scalar values	NMDA/ LGI1: RAVLT, RWFT RRMS: BRB-N, SRT All: BDI-II	NMDA LH scalar 0.9 (*P* =0.001) RH scalar 0.6 (*P* = 0.070) RRMS LH scalar 0.8 (*P* = 0.003) RH scalar 0.6 (*P* = 0.071) LGI1 LH scalar 0.8 (*P* = 0.003) RH scalar 0.9 (*P* = 0.002)	NMDA RAVLT scalar r = 0.335 (*P* = 0.035) RWFT scalar r = –0.033 (*P* = 0.432) BDI-II scalar r_s = –0.100 (*P* = 0.356) RRMS BRB-N Scalar r = 0.540 (*P* = 0.010) LGI1 RAVLT LH Scalar r = 0.348 (*P* = 0.041)—No such obs in controls
Rocca et al. 2015 [70]	MS	BMS (*n* = 26; 0.44 (7) yrs (SD); 18 F RRMS (*n* = 28; 0.40 (11) yrs (SD); 20 F SPMS (*n* = 34; 0.46 (11) yrs (SD); 24 F HC (*n* = 28; 0.45 (11); 0.18 F	MRI	Manual tracing (MNI) space	Mesh modelling	Post MRI: vertex based analysis: radial dist. (DG)	WL test, SS test	BMS Lt DG rad dist 0.6 (*P* = NS) Rt DG no vertices (*P* = NS) RRMS Lt DG rad dist 0.8 (*P* = NS) Rt DG Rad Dist 0.7 (*P* = NS) SPMS Lt DG Rad Dist 0.7 (*P* = NS) Rt DG Rad Dist 0.6 (*P* = NS)	BMS WL Lt DG rad dist r = –0.43 (*P* = NS) RRMS WL Lt DG rad dist r = 0.50 (*P* = NS) SS Lt DG Rad Dist r = 0.47 (*P* = NS) SPMS WL Lt DG Rad Dist r = –0.41 (*P* = NS) SS Lt DG Rad Dist r = –0.38 (*P* = NS) WL Rt DG Rad Dist r = –0.39 (*P* = NS)
Cacciaguerra et al. 2019 [71]	MS	CIS (*n* = 36; 0.31 (7) yrs (SD); 29 F HC (*n* = 14; 0.34 (8) yrs (SD); 10 F	MRI	Manual tracing (MNI) Space	Mesh modelling	Post MRI: Radial mapping analysis: radial dist. HSRV (CA1, presubiculum, CA4, DG)	PASAT	CIS (M3) Rt CA1 HSRV 0.2 (*P* = 0.009) Rt mol layer HSRV 0.1 (*P* = 0.003) Rt gran layer DG HSRV 0.2 (*P* = 0.002) Rt Presubiculum HSRV 0.3 (*P* = 0.026) Rt CA4 HSRV 0.3 (*P* = 0.007)	Nwo correlation with PASAT

(CVLT) scores in MS and CIS, respectively, and was also able to effectively discriminate between memory impaired and memory preserved patients with CIS. In contrast, a decrease in the FA parameter had positive correlations with SDMT [65]. Negative correlations were observed with the following: BBB parameters in SLE and elevated MD in AE correlated with varying neuropsychological assessment scores.

(Automated Neuropsychological Assessment Metrics (ANAM); Ray Auditory Verbal Learning Test (RAVLT), and Rey–Osterrieth Complex Figure (ROCF) respectively) [50] [67, 68]. There were also correlations observed with imaging measures and scores on the affective scales in MS and SLE patients. TSPO hippocampal distribution volume ratio in MS and BBB parameters in SLE were positively correlated with BDI scores [25, 50]. Decrease FA parameter correlated with HAMD scores [69].

In the second group of studies examining separate hippocampal subfields and reporting neurodegenerative changes due to neuroinflammation, we included three studies using MESH modelling. Regional changes were detected between subfields. In MS patients there was the surface expansion of the hippocampal dentate gyrus (DG) as measured by radial distance (RD) enlargement [70]. This was also observed in the study by Cacciaguera *et al.* [71], looking at serial regional measurements, with surface expansion more pronounced in later months. In contrast, there was a reduction in RD in the CA1 subfield after 3 months of progressing to the subiculum. Across MS and AE, deformation overlap corresponded to damage within the CA1 subfield [72].

Discussion

Our systematic review of the literature focused on imaging measures of hippocampal neuroinflammation in three prototypical autoimmune neuroinflammatory conditions. It revealed the largest and most consistent significant differences between cases and controls in MS patients, particularly those with the more progressive forms, as shown by studies using TSPO PET and DW MRI. Preliminary results from studies employing other techniques, such as susceptibility, MTR, and DCE, appeared promising but require replication in larger samples.

All studies reported global hippocampal imaging measures, and no information specifically related to immunocompetent cell density (e.g. TSPO) or microstructural integrity (e.g. DWI) was reported for separate hippocampal subfields. Although two studies in AE depicted individual sub-regional atrophy in CA1, CA2/CA3, CA4/DG, and in the subicula regions of the hippocampus, diffusion changes were only reported in the hippocampus as a whole. Our separate analysis looking at the effect on morphological changes, resulting from neurodegeneration, in neuroinflammatory conditions, confirmed our predicted differential vulnerability of subfields to inflammation. For instance, there were specific contrasting measurements in radial distance observed between DG and CA1.

The value of correlations to functional deficits and clinical manifestation were limited by small samples but overall provided preliminary evidence that signs of hippocampal neuroinflammation, capable of causing functional alterations such as processing speed, semantic organization, attention, concentration, visuospatial constructional ability, depression and anxiety, might be detected using quantitative imaging markers [73, 74, 66, 25].

Although these correlational data suggest that these quantitative imaging measures are potentially related to clinical phenomena, the lack of specific correspondence between imaging signals and underlying histopathology limits their precise interpretability. For instance, although a large proportion of the TSPO PET signal increases observed in the acute phase of inflammation in MS can be attributed to an increased density of TSPO expressing macrophages/microglia resulting from their infiltration, proliferation, and activation [41, 42]; it is possible that as time progresses, astrocytes contribute to an increasingly substantial proportion of observed hippocampal signal [75]. The discrepancy between findings in MS relative to SLE studies might reflect unique and disease-specific changes in constitutive binding to TSPO expressed by non-inflammatory cells (including for example platelets, endothelia, or other TSPO expressing peripheral cell types), which might be particularly relevant to conditions with systemic and generalized inflammatory responses such as SLE.

Furthermore, TSPO PET presents challenges to quantification of the specific radiotracer binding which becomes particularly difficult to address in presence of systemic inflammatory responses [76] and might contribute to the variability of results between studies due to inconsistencies in methodological approaches.

DW MRI was frequently utilized especially in MS. The specificity of its applications and the extent to which it captures and quantifies hippocampal microstructural alterations in neuro-inflammatory pathology have been frequently investigated using pre-clinical and experimental models. Göbel-Guéniot *et al.* [77] observed CA1 pyramidal cell degeneration and granular cell layer dispersions correlated significantly with alterations in tissue diffusivity parameters in murine models of Mesial temporal lobe epilepsy (MTLE), a common type of epilepsy affecting inner aspects of the temporal lobes, which can present in the hippocampus. The findings support the capability of high-resolution DW MRI in measuring quantitative changes in epileptic hippocampal tissue consistent with histopathological features in MTLE. Crombe [18] assessed two diffusion-related imaging measures (DTI and NODDI) in terms of their sensitivity to effectively delineate, compute and quantify microstructural alterations in specific hippocampal layers in mice with EAE, a murine experimental model of RRMS. NODDI employs a multishell tissue modality in the characterization of tissue microstructure while DTI is a simpler approach that assumes a single water compartment characterized by anisotropic diffusion. Both modalities were equally effective in delineating specific hippocampal layers and the quantification of diffusivity parameters presented differences within three specific layers (stratum radiatum (SR), stratum lacunosum moleculare (SLM), molecular layer (ML)). DTI showed more prospects with regard to quantification. The same study assessed histopathological correlations between EAE pathology and DW-imaging measures and identified a reduction in AD and MD in the molecular layer of the hippocampus of a mouse model of EAE, corresponding histologically to microglial activation and a reduction in dendritic density, consistent with early neuroinflammatory and neurodegenerative processes respectively. This interestingly contrasts with the findings of the studies we reviewed here, where both MS and AE were associated with increased

hippocampal MD across studies. A logical explanation here may indeed be due to progression from the MD reduction, reflecting the early neuroinflammatory and neurodegenerative disease processes characteristic of EAE, to more sustained and progressive neurodegenerative pathology seen in MS patients where the expansion of extracellular fluid and microscopic barrier disruptions become progressively more prominent [67]. Similar distinctive observations were a sole reduction in FA in Clinically isolated syndrome (CIS), considered the first neurological onset of potential MS, and an additional increase in MD seen in MS patients [65]. However, the impact of partial volume effects with CSF should not be excluded, as human MRI data are typically acquired with much lower resolution.

Due to indirect measures between tissue architecture and DW parameters, DW MRI does lack levels of specificity in neuroinflammatory pathology [18]. Both MD and FA are sensitive to increases in extracellular water, reduction in myelin, changes in microstructure, and changes in cell density. It is therefore difficult to associate the observed changes with a specific pathological substrate. More so, human applications have also revealed considerable limitations in acquisition due to low-resolution protocols specifically designed for the whole brain [78]. To mitigate these effects and limitations, Treit developed a simple DTI protocol that employed standard single-shot 2D Echo-planar imaging (EPI) at 3T, to obtain high spatial resolution images ($1 \times 1 \times 1$ mm^3) of the human hippocampus. To compensate for the SNR loss induced by the small voxels, they proposed to use a relatively low *b*-value (thus reducing the amount of diffusion weighting), at the price of limiting the sensitivity to the microscopic water environment. This may potentially decrease or limit the certainty of identifying vital micro-image details in neuroinflammatory pathology, in an already complex structure such as the hippocampus.

There are other notable methodological concerns in processing hippocampal neuroinflammatory imaging data, which may arise post-MRI acquisition such as proposed methods of segmentation, risk of poor precision in co-registration of DW maps if segmentation is done on T1, and resolution limits that can effectively distinguish hippocampal subfields or layers. DW MRI is typically acquired using echo-planar imaging [79], a pulse sequence insensitive to bulk motion, but characterized by geometric distortions induced by magnetic susceptibility [80]. As a consequence, the anatomy on DW EPI does not match the corresponding T1-weighted scans, making image coregistration between the two modalities challenging.

Even if perfect coregistration could be achieved, due to the morphological complexities and extremely small structural sizes of the hippocampal compartments, segmenting the subregions of the hippocampus is indeed fraught with difficulties and immense challenges in the analysis of MRI images [81]. Hippocampal segmentation might be obtained by either automated or manual methods: most of the studies included in our review have utilized automated methods, such as FSL and Free Surfer. Only the studies by Rocca *et al*. [70] and Cacciaguerra *et al*. [71] employed manual tracing for hippocampal segmentation. While manual segmentation by adequately trained human raters is generally regarded as the gold standard [82], semi-automated and more automatic methods appear to be gaining traction with a view to reducing workload, increasing reproducibility, and avoiding inter/intra-rater variability which is also common with manual methods of segmentation. Automated methods are however not without limitations, which range from a lack of public availability, being subject to error in significant disease states, and requiring parameter tuning [83].

Taking resolution into consideration, a future approach could be computational imaging techniques, which enhance the contrast and resolution of lower-resolution images. One such application is the image quality transfer (IQT) approach, which mitigates the challenges resulting from spatial resolution, lengthy acquisition protocols, slow translation, interpolation, and complex processing pipelines. IQT technique adapts clinically low-quality mappings to experimental high-quality images applying the likeness of images across scales, modalities, regions, and subjects [84]. With the avoidance of artefacts comprising hot-spots and blurring, and the reduction of partial volume effects, finer details are recovered that were lost at low resolution, hence, allowing for easier identification of hippocampal architecture including morphology, digitations, landmarks, boarders, and separation of sub-regional layers. Zooming into the desired region (medial temporal lobe for instance) allows for adequate manual segmentation directly on diffusion images, with subsequent computation of desirable diffusion parameters. The need for co-registration to anatomical or histological images is hence diminished.

The poor specificity of diffusion MRI is caused by its sensitivity to all water compartments (intra- and extra-cellular). A way to overcome this limitation is by combining the sensitivity to microstructure offered by diffusion MRI with the cell-specificity of MRS. Diffusion-weighted MRS (DW-MRS) offers a promising and cheaper alternative for non-invasively characterizing the effects of inflammation in the brain [28]. In De Marco's study, DW-MRS was able to provide cell-specific information about cellular morphology and equally, was found sensitive to systemic inflammation-induced glial cytomorphological changes in grey matter [28]. It should be re-iterated, however, that the hippocampus is an exceptionally challenging region to capture with this technique, which is inherently characterized by very poor spatial resolution.

Conclusion

In our review, we explained why the hippocampus is an important site of neuroinflammation and highlighted possible reasons underlying its vulnerability, which differentially affects hippocampal subfields. We also reported challenges associated with the application of hippocampal imaging of neuroinflammation using both conventional and novel imaging techniques. Our review did provide confirmatory evidence that a few imaging markers that reflect neuroinflammatory tissue changes, such as DW-MRI and TSPO PET, were able to detect signal alterations in the hippocampus in prototypical neuroinflammatory conditions. However, no study as yet has examined hippocampal subfields separately.

We propose that this could be addressed by the use of higher resolution acquisitions, or alternatively the adoption of particular post-processing techniques, which represent promising approaches to gain better insight into neuroinflammatory pathology *in vivo*, ultimately enabling more precise and sensitive characterization of hippocampal pathophysiology.

Supplementary data

Supplementary data is available at *Clinical and Experimental Immunology* online.

Acknowledgements

The authors would like to appreciate the efforts of all research participants with autoimmune inflammatory conditions including MS, SLE, and AE.

Funding

There was no external funding support for this study

Conflict of interests

Dr Prince Nwaubani has no conflict of interest or competing interests to disclose. Prof Mara Cercignani has no conflict of interest or competing interests to disclose. Dr Alessandro Colasanti has no conflict of interest or competing interests to disclose.

Author contributions

Data were extracted by Dr Nwaubani and later reviewed by Dr Colasanti and Prof Cercignani. The quality of each study included was independently assessed by Dr Colasanti and Prof Cercignani. Write up of the article was done by all three authors.

Data availability

Since this is a systematic review article of the available literature, data sharing is not applicable to this article as no new data were created or analyzed in this study.

References

1. Anand KS, Dhikav V. Hippocampus in health and disease: an overview. *Ann Indian Acad Neurol* 2012, 15, 239–46. doi:10.4103/0972-2327.104323.
2. Papadopoulos D, Dukes S, Patel R, Nicholas R, Vora A, Reynolds R. Substantial archaeocortical atrophy and neuronal loss in multiple sclerosis. *Brain Pathol* 2009, 19, 238–53. doi:10.1111/j.1750-3639.2008.00177.x.
3. Geurts JJ, Bö L, Roosendaal SD, Hazes T, Daniëls R, Barkhof F, et al. Extensive hippocampal demyelination in multiple sclerosis. *J Neuropathol Exp Neurol* 2007, 66, 819–27.
4. Dutta R, Chang A, Doud MK, Kidd GJ, Ribaudo MV, Young EA, et al. Demyelination causes synaptic alterations in hippocampi from multiple sclerosis patients. *Ann Neurol* 2011, 69, 445–54. doi:10.1002/ana.22337.
5. Nisticò R, Mango D, Mandolesi G, Piccinin S, Berretta N, Pignatelli M, et al. Inflammation subverts hippocampal synaptic plasticity in experimental multiple sclerosis. *PLoS One* 2013, 8, e54666. doi:10.1371/journal.pone.0054666.
6. Williamson LL, Bilbo SD. Chemokines and the hippocampus: a new perspective on hippocampal plasticity and vulnerability. *Brain Behav Immun* 2013, 30, 186–94. doi:10.1016/j.bbi.2013.01.077.
7. McEwen BS, de Leon MJ, Lupien SJ, Meaney MJ. Corticosteroids, the aging brain and cognition. *Trends Endocrinol Metab* 1999, 10, 92–6.
8. Marques F, Sousa JC, Coppola G, Falcao AM, Rodrigues AJ, Geschwind DH, et al. Kinetic profile of the transcriptome changes induced in the choroid plexus by peripheral inflammation. *J Cereb Blood Flow Met* 2009, 29, 921–32.
9. Brown DA, Sawchenko PE. Time course and distribution of inflammatory and neurodegenerative events suggest structural bases for the pathogenesis of experimental autoimmune encephalomyelitis. *J Comp Neurol* 2007, 502, 236–60.
10. Reboldi A, Coisne C, Baumjohann D, Benvenuto F, Bottinelli D, Lira S, et al. CC chemokine receptor 6–regulated entry of T H-17 cells into the CNS through the choroid plexus is required for the initiation of EAE. *Nat Immunol* 2009, 10, 514–23. doi:10.1038/ni.1716.
11. Farrar WL, Hill JM, Harel-Bellan A, Vinocour M. The immune logical brain. *Immunol Rev* 1987, 100, 361–78.
12. Fukushima S, Furube E, Itoh M, Nakashima T, Miyata S. Robust increase of microglia proliferation in the fornix of hippocampal axonal pathway after a single LPS stimulation. *J Neuroimmunol* 2015, 285, 31–40. doi:10.1016/j.jneuroim.2015.05.014.
13. Pérez-Rodríguez DR, Blanco-Luquin I, Mendioroz M. The participation of microglia in neurogenesis: a review. *Brain Sci* 2021, 11, 658. doi:10.3390/brainsci11050658.
14. Ming GL, Song H. Adult neurogenesis in the mammalian central nervous system. *Annu Rev Neurosci* 2005, 28, 223–50. doi:10.1146/annurev.neuro.28.051804.101459.
15. Valero J, Bernardino L, Cardoso FL, Silva AP, Fontes-Ribeiro C, Ambrósio AF, et al. Impact of neuroinflammation on hippocampal neurogenesis: relevance to aging and Alzheimer's disease. *J Alzheimer's Dis* 2017, 60, S161–8. doi:10.3233/jad-170239.
16. Anacker C. Adult hippocampal neurogenesis in depression: behavioral implications and regulation by the stress system. *Behav Neurobiol Stress-Related Dis* 2014, 25–43.
17. Campbell IL, Erta M, Lim SL, Frausto R, May U, Rose-John S, et al. Trans-signaling is a dominant mechanism for the pathogenic actions of interleukin-6 in the brain. *J Neurosci* 2014, 34, 2503–13. doi:10.1523/jneurosci.2830-13.2014.
18. Crombe A, Planche V, Raffard G, Bourel J, Dubourdieu N, Panatier A, et al. Deciphering the microstructure of hippocampal subfields with in vivo DTI and NODDI: applications to experimental multiple sclerosis. *Neuroimage* 2018, 172, 357–68. doi:10.1016/j.neuroimage.2018.01.061.
19. Perosa V, Priester A, Ziegler G, Cardenas-Blanco A, Dobisch L, Spallazzi M, et al. Hippocampal vascular reserve associated with cognitive performance and hippocampal volume. *Brain* 2020, 143, 622–34. doi:10.1093/brain/awz383.
20. Shaw K, Bell L, Boyd K, Grijseels DM, Clarke D, Bonnar O, et al. Neurovascular coupling and oxygenation are decreased in hippocampus compared to neocortex because of microvascular differences. *Nat Commun* 2021, 12, 1–6.
21. Bartsch T, Schönfeld R, Müller FJ, Alfke K, Leplow B, Aldenhoff J, et al. Focal lesions of human hippocampal CA1 neurons in transient global amnesia impair place memory. *Science* 2010, 328, 1412–5. doi:10.1126/science.1188160.
22. Bartsch T, Döhring J, Reuter S, Finke C, Rohr A, Brauer H, et al. Selective neuronal vulnerability of human hippocampal CA1 neurons: lesion evolution, temporal course, and pattern of hippocampal damage in diffusion-weighted MR imaging. *J Cereb Blood Flow Met.* 2015, 35, 1836–45.
23. Pinna A, Colasanti A. The neurometabolic basis of mood instability: the parvalbumin interneuron link—a systematic review and meta-analysis. *Front Pharmacol* 2021, 2324. doi:10.3389/fphar.2021.689473
24. Albrecht DS, Granziera C, Hooker JM, Loggia ML. In vivo imaging of human neuroinflammation. *ACS Chem Neurosci* 2016, 7, 470–83. doi:10.1021/acschemneuro.6b00056.
25. Colasanti A, Guo Q, Giannetti P, Wall MB, Newbould RD, Bishop C, et al. Hippocampal neuroinflammation, functional connectivity, and depressive symptoms in multiple sclerosis. *Biol Psychiatry* 2016, 80, 62–72. doi:10.1016/j.biopsych.2015.11.022.
26. Lee Y, Park Y, Nam H, Lee JW, Yu SW. Translocator protein (TSPO): the new story of the old protein in neuroinflammation. *BMB Rep* 2020, 53, 20.

27. Herrera-Rivero M, Heneka MT, Papadopoulos V. Translocator protein and new targets for neuroinflammation. *Clin Trans Imaging* 2015, 3, 391–402. doi:10.1007/s40336-015-0151-x.
28. De Marco R, Ronen I, Branzoli F, Amato ML, Asllani I, Colasanti A, et al. Diffusion-weighted MR spectroscopy (DW-MRS) is sensitive to LPS-induced changes in human glial morphometry: a preliminary study. *Brain Behav Immun* 20221, 99, 256–65. doi:10.1016/j.bbi.2021.10.005.
29. Pereira JB, Valls-Pedret C, Ros E, Palacios E, Falcón C, Bargalló N, Bartrés-Faz D, Wahlund LO, Westman E, Junque C. Regional vulnerability of hippocampal subfields to aging measured by structural and diffusion MRI. *Hippocampus* 2014, 24, 403–14.
30. Zheng F, Cui D, Zhang L, Zhang S, Zhao Y, Liu X, et al. The volume of hippocampal subfields in relation to decline of memory recall across the adult lifespan. *Front Aging Neurosci* 2018, 320. doi:10.3389/fnagi.2018.00320
31. Ferrucci L, Fabbri E. Inflammageing: chronic inflammation in ageing, cardiovascular disease, and frailty. *Nat Rev Cardiol* 2018, 15, 505–22. doi:10.1038/s41569-018-0064-2.
32. Yegorov YE, Poznyak AV, Nikiforov NG, Sobenin IA, Orekhov AN. The link between chronic stress and accelerated aging. *Biomedicines* 2020, 8, 198. doi:10.3390/biomedicines8070198.
33. Sormani MP, Bonzano L, Roccatagliata L, Cutter GR, Mancardi GL, Bruzzi P. Magnetic resonance imaging as a potential surrogate for relapses in multiple sclerosis: a meta-analytic approach. *Ann Neurol* 2009, 65, 268–75.
34. Arnold DL, Matthews PM. MRI in the diagnosis and management of multiple sclerosis. *Neurology* 2002, 58, S23–31. doi:10.1212/wnl.58.8_suppl_4.s23.
35. Peterson JW, Bö L, Mörk S, Chang A, Trapp BD. Transected neurites, apoptotic neurons, and reduced inflammation in cortical multiple sclerosis lesions. *Ann Neurol* 2001, 50, 389–400.
36. Owen DR, Narayan N, Wells L, Healy L, Smyth E, Rabiner EA, et al. Pro-inflammatory activation of primary microglia and macrophages increases 18 kDa translocator protein expression in rodents but not humans. *J Cereb Blood Flow Met* 2017, 37, 2679–90.
37. Notter T, Schalbetter SM, Clifton NE, Mattei D, Richetto J, Thomas K, et al. Neuronal activity increases translocator protein (TSPO) levels. *Mol Psychiat* 2021, 26, 2025–37. doi:10.1038/s41380-020-0745-1.
38. Vicente-Rodríguez M, Singh N, Turkheimer F, Peris-Yague A, Randall K, Veronese M, et al. Resolving the cellular specificity of TSPO imaging in a rat model of peripherally-induced neuroinflammation. *Brain Behav Immun* 2021, 96, 154–67.
39. Chen MK, Guilarte TR. Translocator protein 18 kDa (TSPO): molecular sensor of brain injury and repair. *Pharmacol Ther* 2008, 118, 1–17. doi:10.1016/j.pharmthera.2007.12.004.
40. Venneti S, Lopresti BJ, Wiley CA. The peripheral benzodiazepine receptor (translocator protein 18 kDa) in microglia: from pathology to imaging. *Prog Neurobiol* 2006, 80, 308–22. doi:10.1016/j.pneurobio.2006.10.002.
41. Nutma E, Stephenson JA, Gorter RP, de Bruin J, Boucherie DM, Donat CK, et al. A quantitative neuropathological assessment of translocator protein expression in multiple sclerosis. *Brain* 2019, 142, 3440–55. doi:10.1093/brain/awz287.
42. Nutma E, Ceyzériat K, Amor S, Tsartsalis S, Millet P, Owen DR, et al. Cellular sources of TSPO expression in healthy and diseased brain. *Eur J Nucl Med Mol Imaging* 2021, 12, 1–8.
43. Kim MJ, Lee JH, Juarez Anaya F, Hong J, Miller W, Telu S, et al. First-in-human evaluation of [11C] PS13, a novel PET radioligand, to quantify cyclooxygenase-1 in the brain. *Eur J Nucl Med Mol Imaging* 2020, 47, 3143–51. doi:10.1007/s00259-020-04855-2.
44. Rodriguez-Vieitez E, Nordberg A. Imaging neuroinflammation: quantification of astrocytosis in a multitracer PET approach. In *Biomarkers for Alzheimer's Disease Drug Development* 2018 (pp. 231–251). New York, NY: Humana Press.
45. Calsolaro V, Matthews PM, Donat CK, Livingston NR, Femminella GD, Guedes SS, et al. Astrocyte reactivity with late-onset cognitive impairment assessed in vivo using 11C-BU99008 PET and its relationship with amyloid load. *Mol Psychiatry* 2021, 15, 1–8.
46. Tognarelli JM, Dawood M, Shariff MI, Grover VP, Crossey MM, Cox IJ, et al. Magnetic resonance spectroscopy: principles and techniques: lessons for clinicians. *JCEH*. 2015, 5, 320–8. doi:10.1016/j.jceh.2015.10.006.
47. Kermode AG, Thompson AJ, Tofts P, MacManus DG, Kendall BE, Kingsley DP, et al. Breakdown of the blood–brain barrier precedes symptoms and other MRI signs of new lesions in multiple sclerosis: pathogenetic and clinical implications. *Brain* 1990, 113, 1477–89.
48. Starr JM, Farrall AJ, Armitage P, McGurn B, Wardlaw J. Blood–brain barrier permeability in Alzheimer's disease: a case–control MRI study. *Psychiatry Res Neuroimaging* 2009, 171, 232–41. doi:10.1016/j.pscychresns.2008.04.003.
49. Ibrahim MA, Hazhirkarzar B, Dublin AB. Gadolinium magnetic resonance imaging. In: *StatPearls*. Treasure Island, FL: StatPearls Publishing, 2021.
50. Chi JM, Mackay M, Hoang A, Cheng K, Aranow C, Ivanidze J, et al. Alterations in blood–brain barrier permeability in patients with systemic lupus erythematosus. *Am J Neuroradiol* 2019, 40, 470–7.
51. de Figueiredo EH, Borgonovi AF, Doring TM. Basic concepts of MR imaging, diffusion MR imaging, and diffusion tensor imaging. *Magn Reson Imaging Clin* 2011, 19, 1–22.
52. Basser PJ, Mattiello J, LeBihan D. MR diffusion tensor spectroscopy and imaging. *Biophys J* 1994, 66, 259–67. doi:10.1016/S0006-3495(94)80775-1.
53. Winklewski PJ, Sabisz A, Naumczyk P, Jodzio K, Szurowska E, Szarmach A. Understanding the physiopathology behind axial and radial diffusivity changes—what do we know?. *Front Neurol* 2018, 9, 92. doi:10.3389/fneur.2018.00092.
54. Zhang H, Schneider T, Wheeler-Kingshott CA, Alexander DC. NODDI: practical in vivo neurite orientation dispersion and density imaging of the human brain. *Neuroimage* 2012, 61, 1000–16. doi:10.1016/j.neuroimage.2012.03.072.
55. Cercignani M, Bozzali M, Iannucci G, Comi G, Filippi M. Magnetisation transfer ratio and mean diffusivity of normal appearing white and grey matter from patients with multiple sclerosis. *J Neurol Neurosurg Psychiat* 2001, 70, 311–7.
56. Serres S, Anthony DC, Jiang Y, Broom KA, Campbell SJ, Tyler DJ, et al. Systemic inflammatory response reactivates immune-mediated lesions in rat brain. *J Neurosci* 2009, 29, 4820–8. doi:10.1523/jneurosci.0406-09.2009.
57. Stanisz GJ, Webb S, Munro CA, Pun T, Midha R. MR properties of excised neural tissue following experimentally induced inflammation. *Magn Reson Med* 2004, 51, 473–9.
58. Pain CC, Piggott MD, Goddard AJ, Fang F, Gorman GJ, Marshall DP, et al. Three-dimensional unstructured mesh ocean modelling. *Ocean Modell* 2005, 10, 5–33.
59. Moher D, Liberati A, Tetzlaff J, Altman DG; PRISMA Group. Preferred reporting items for systematic reviews and meta-analyses: the PRISMA statement. *Ann Intern Med* 2009, 151, 264–9, W64. doi:10.7326/0003-4819-151-4-200908180-00135.
60. Hughes EG, Peng X, Gleichman AJ, Lai M, Zhou L, Tsou R, et al. Cellular and synaptic mechanisms of anti-NMDA receptor encephalitis. *J Neurosci* 2010, 30, 5866–75. doi:10.1523/jneurosci.0167-10.2010.
61. Ballok DA, Woulfe J, Sur M, Cyr M, Sakic B. Hippocampal damage in mouse and human forms of systemic autoimmune disease. *Hippocampus* 2004, 14, 649–61. doi:10.1002/hipo.10205.
62. Schnider A, Bassetti C, Gutbrod K, Ozdoba C. Very severe amnesia with acute onset after isolated hippocampal damage due to systemic lupus erythematosus. *J Neurol Neurosurg Psychiatry* 1995, 59, 644.
63. Herranz E, Giannì C, Louapre C, Treaba CA, Govindarajan ST, Ouellette R, et al. Neuroinflammatory component of gray matter pathology in multiple sclerosis. *Ann Neurol* 2016, 80, 776–90. doi:10.1002/ana.24791.

64. Cappellani R, Bergsland N, Weinstock-Guttman B, Kennedy C, Carl E, Ramasamy DP, et al. Subcortical deep gray matter pathology in patients with multiple sclerosis is associated with white matter lesion burden and atrophy but not with cortical atrophy: a diffusion tensor MRI study. *Am J Neuroradiol* 2014, 35, 912–9.
65. Planche V, Ruet A, Coupé P, Lamargue-Hamel D, Deloire M, Pereira B, et al. Hippocampal microstructural damage correlates with memory impairment in clinically isolated syndrome suggestive of multiple sclerosis. *Mult Scler J* 2017, 23, 1214–24.
66. Vrenken H, Pouwels PJ, Ropele S, Knol DL, Geurts JJ, Polman CH, et al. Magnetization transfer ratio measurement in multiple sclerosis normal-appearing brain tissue: limited differences with controls but relationships with clinical and MR measures of disease. *Mult Scler J* 2007, 13, 708–16.
67. Finke C, Kopp UA, Pajkert A, Behrens JR, Leypoldt F, Wuerfel JT, et al. Structural hippocampal damage following anti-N-methyl-D-aspartate receptor encephalitis. *Biol Psychiat* 2016, 79, 727–34. doi:10.1016/j.biopsych.2015.02.024.
68. Finke C, Prüss H, Heine J, Reuter S, Kopp UA, Wegner F, et al. Evaluation of cognitive deficits and structural hippocampal damage in encephalitis with leucine-rich, glioma-inactivated 1 antibodies. *JAMA Neurol* 2017, 74, 50–9.
69. Shen Y, Bai L, Gao Y, Cui F, Tan Z, Tao Y, et al. Depressive symptoms in multiple sclerosis from an in vivo study with TBSS. *Biomed Res Int* 2014, 2014, 1–8. doi:10.1155/2014/148465.
70. Rocca MA, Longoni G, Pagani E, Boffa G, Colombo B, Rodegher M, et al. In vivo evidence of hippocampal dentate gyrus expansion in multiple sclerosis. *Hum Brain Mapp* 2015, 36, 4702–13. doi:10.1002/hbm.22946.
71. Cacciaguerra L, Pagani E, Mesaros S, Dackovic J, Dujmovic-Basuroski I, Drulovic J, et al. Dynamic volumetric changes of hippocampal subfields in clinically isolated syndrome patients: a 2-year MRI study. *Mult Scler J* 2019, 25, 1232–42.
72. Heine J, Prüß H, Scheel M, Brandt AU, Gold SM, Bartsch T, et al. Transdiagnostic hippocampal damage patterns in neuroimmunological disorders. *NeuroImage Clin* 2020, 28, 102515. doi:10.1016/j.nicl.2020.102515.
73. Filip P, Svatkova A, Carpenter AF, Eberly LE, Nestrasil I, Nissi MJ, et al. Rotating frame MRI relaxations as markers of diffuse white matter abnormalities in multiple sclerosis. *NeuroImage Clin* 2020, 26, 102234. doi:10.1016/j.nicl.2020.102234.
74. Geurts JJ, Reuling IE, Vrenken H, Uitdehaag BM, Polman CH, Castelijns JA, et al. MR spectroscopic evidence for thalamic and hippocampal, but not cortical, damage in multiple sclerosis. *Magn Reson Med* 2006, 55, 478–83.
75. Nguyen DL, Wimberley C, Truillet C, Jego B, Caillé F, Pottier G, et al. Longitudinal positron emission tomography imaging of glial cell activation in a mouse model of mesial temporal lobe epilepsy: toward identification of optimal treatment windows. *Epilepsia* 2018, 59, 1234–44. doi:10.1111/epi.14083.
76. Woodcock EA, Schain M, Cosgrove KP, Hillmer A. Quantification of [11C] PBR28 data after systemic lipopolysaccharide challenge. *EJNMMI Res* 2020, 10, 1–6.
77. Göbel-Guéniot K, Gerlach J, Kamberger R, Leupold J, Von Elverfeldt D, Hennig J, et al. Histological correlates of diffusion-weighted magnetic resonance microscopy in a mouse model of mesial temporal lobe epilepsy. *Front Neurosci* 2020, 543. doi:10.3389/fnins.2020.00543
78. Treit S, Steve T, Gross DW, Beaulieu C. High resolution in-vivo diffusion imaging of the human hippocampus. *Neuroimage* 2018, 182, 479–87. doi:10.1016/j.neuroimage.2018.01.034.
79. Schmitt F. Echo-planar imaging. In: *Brain Mapping: An Encyclopedic Reference*; 2015.
80. Brun L, Pron A, Sein J, Deruelle C, Coulon O. Diffusion MRI: assessment of the impact of acquisition and preprocessing methods using the BrainVISA-diffuse toolbox. *Front Neurosci* 2019, 536. doi:10.3389/fnins.2019.00536
81. Shi Y, Cheng K, Liu Z. Hippocampal subfields segmentation in brain MR images using generative adversarial networks. *Biomed Eng Online* 2019, 18, 1–2.
82. Dalton MA, Zeidman P, Barry DN, Williams E, Maguire EA. Segmenting subregions of the human hippocampus on structural magnetic resonance image scans: an illustrated tutorial. *Brain Neurosci Adv* 2017, 1, 2398212817701448. doi:10.1177/2398212817701448.
83. Goubran M, Ntiri EE, Akhavein H, Holmes M, Nestor S, Ramirez J, Adamo S, et al. *Hippocampal Segmentation for Brains with Extensive Atrophy using Three-Dimensional Convolutional Neural Networks*. Hoboken, USA: John Wiley & Sons, Inc.; 2020.
84. Alexander DC, Zikic D, Ghosh A, Tanno R, Wottschel V, Zhang J, et al. Image quality transfer and applications in diffusion MRI. *NeuroImage* 2017, 152, 283–98. doi:10.1016/j.neuroimage.2017.02.089.
85. Singhal T, O'Connor K, Dubey S, Pan H, Chu R, Hurwitz S, et al. Gray matter microglial activation in relapsing vs progressive MS: A [F-18] PBR06-PET study. *Neurol-Neuroimmunol* 2019, 6, e587. doi:10.1212/NXI.0000000000000587
86. Roosendaal SD, Hulst HE, Vrenken H, Feenstra HE, Castelijns JA, Pouwels PJ, et al. Structural and functional hippocampal changes in multiple sclerosis patients with intact memory function. *Radiology* 2010, 255, 595–604. doi:10.1148/radiol.10091433.
87. Yin P, Liu Y, Xiong H, Han Y, Sah SK, Zeng C, et al. Structural abnormalities and altered regional brain activity in multiple sclerosis with simple spinal cord involvement. *Br J Radiol* 2018, 91, 20150777. doi:10.1259/bjr.20150777.
88. Wang Y, Coughlin JM, Ma S, Endres CJ, Kassiou M, Sawa A, et al. Neuroimaging of translocator protein in patients with systemic lupus erythematosus: a pilot study using [11C] DPA-713 positron emission tomography. *Lupus* 2017, 26, 170–8. doi:10.1177/0961203316657432.
89. Appenzeller S, Carnevalle AD, Li LM, Costallat LT, Cendes F. Hippocampal atrophy in systemic lupus erythematosus. *Ann Rheum Dis* 2006, 65, 1585–9. doi:10.1136/ard.2005.049486.
90. Zrzavy T, Endmayr V, Bauer J, Macher S, Mossaheb N, Schwaiger C, et al. Neuropathological variability within a spectrum of NMDAR-encephalitis. *Ann Neurol* 2021, 90, 725–37. doi:10.1002/ana.26223.
91. Dekeyzer S, De Kock I, Nikoubashman O, Vanden Bossche S, Van Eetvelde R, De Groote J, et al. "Unforgettable"—a pictorial essay on anatomy and pathology of the hippocampus. *Insights Imaging* 2017, 8, 199–212. doi:10.1007/s13244-016-0541-2.